Cancer Chemother Pharmacol (2011) 68:349–358
DOI 10.1007/s00280-010-1464-0

ORIGINAL ARTICLE

Anticancer effect of (*E*)-2-hydroxy-3′,4,5′-trimethoxystilbene on breast cancer cells by mitochondrial depolarization

Yee Soo Chae · Jong Gwang Kim · Hyun Jun Jung · Jung Dug Yang · Jin Hyang Jung · Sarah E. Aiyar · Sanghee Kim · Hoyong Park

Received: 11 July 2010 / Accepted: 6 September 2010 / Published online: 27 October 2010

Abstract
Background TMS (2,3′,4,5′-tetramethoxystilbene), a stilbene analog derived from rhapontigenin, was previously demonstrated to induce apoptosis in hormone-resistant breast cancer cells. Therefore, this study investigated the anticancer effect of a new stilbene analog, HTMS ((*E*)-2-hydroxy-3′,4,5′-trimethoxystilbene), and its mechanism in various breast cancer cell lines.
Materials and methods The effect of HTMS on cell proliferation of MDA-MB-231, MCF-7, and LTED cells was evaluated using MTT assays. Cell apoptosis was detected by FITC-annexin V staining and flow cytometry analysis, changes in mitochondrial potential were determined by fluorescence microscopy using TMRE staining, and the expression of cleaved PARP and release of cytochrome *c* were assessed by Western blot analysis.
Results HTMS significantly decreased the cell viability of various types of breast cancer cells in a dose- and time-dependent manner, characterized by G2/M arrest of the cell cycle and the induction of apoptosis. In particular, HTMS disturbed the mitochondrial membrane potential, causing a release of cytochrome *c* during apoptosis. Furthermore, HTMS was superior to TMS in inhibiting cancer cell growth in a pilot comparison study.
Conclusion HTMS is an effective apoptotic agent for breast cancer cells, making it a candidate therapeutic agent for the treatment of breast cancer.

Keywords Stilbene analog · HTMS · Breast cancer · Apoptosis

Abbreviations

DMSO	Dimethylsulfoxide
HTMS	(*E*)-2-Hydroxy-3′,4,5′-trimethoxystilbene
LTED breast cancer	Long-term estradiol-deprived breast cancer
MTT	3-(4,5-Dimethylthiazolyl-2)-2,5-diphenyltetrazoliumbromide
PI	Propidium iodide

Y. S. Chae and H. J. Jung contributed equally to this article as the first authors.

Y. S. Chae · J. G. Kim
Department of Medical Oncology, Kyungpook National University Hospital, Daegu, South Korea

H. J. Jung · H. Park
Cell and Matrix Research Institute, School of Medicine, Kyungpook National University, Daegu, South Korea

H. J. Jung
Department of Biochemistry and Cell Biology, School of Medicine, Kyungpook National University, Daegu, South Korea

J. D. Yang
Department of Plastic surgery, Kyungpook National University Hospital, Daegu, South Korea

J. H. Jung · H. Park (✉)
Department of Surgery, Kyungpook National University Hospital, Samduck-2 Ga, Jung-gu, Daegu 700-721, South Korea
e-mail: phy123@knu.ac.kr

S. E. Aiyar
Department of Internal Medicine, Division of Endocrinology and Metabolism, University of Virginia, Charlottesville, VA, US

S. Kim
College of Pharmacy, Seoul National University, Seoul, South Korea

Rhapontigenin	3,5,3′-Trihydroxy-4′-methoxy-*trans*-stilbene
TMS	2,3′,4,5′-Tetramethoxystilbene

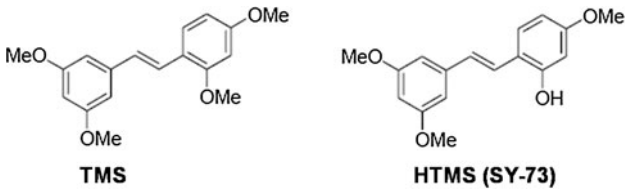

Fig. 1 Chemical structures of TMS and HTMS

Introduction

Breast cancer is the most frequent cause of cancer-related death in women, and despite the availability of diverse systemic treatments, such as hormonal, targeted, and chemotherapeutic agents, metastatic breast cancer at presentation or relapse remains eventually incurable, emphasizing the importance of finding new anticancer compounds with more potent anticancer properties and reduced adverse effects.

Resveratrol (3,5,4′-trihydroxy-trans-stilbene), the most well-known natural stilbenoid [1], exhibits numerous biologic activities, including anti-oxidant [2, 3], antiangiogenic [4], and cancer chemopreventive effects through the inhibition of ribonucleotide reductase and cellular events associated with cell proliferation, tumor initiation, promotion, and progression [5–8]. Furthermore, resveratrol has been shown to have a potent anticancer effect on breast cancer in vitro and in vivo in both ER-positive and ER-negative breast cancer [9–13]. However, it is not a suitable candidate for additional drug development due to its unfavorable pharmacokinetics, such as a short half-life, extensive metabolism, and low bioavailability [14–16]. Therefore, the identification of novel analogs of resveratrol with a better pharmacokinetic profile and chemical stability, yet similar or even stronger biologic activities holds great interest [17–22]. Among the analogs of resveratrol that have already been tested, TMS (2,3′,4,5′-tetramethoxystilbene) has shown a potent and specific inhibitory effect on human CYP450 1A1 and 1B1 enzymes highly over-expressed in several cancer cell lines [23, 24], inducing apoptosis in tamoxifen-resistant (TamR) MCF-7 cells without significant cytotoxicity toward breast epithelial MCF-10A cells [24]. HTMS ((*E*)-2-hydroxy-3′,4,5′-trimethoxystilbene) is structurally very close to TMS, yet possesses a hydroxyl group instead of a 2-methoxy group (Fig. 1). In a previous study, the current authors demonstrated that HTMS preferentially inhibits CYP450 1B1 over 1A1 or 1A2 and has a comparable growth inhibitory effect to that of TMS on human lung (A549) and colon cancer cells (Col2) [21, 25]. Accordingly, this study explored the possible therapeutic potential of HTMS for breast cancer by examining its inhibitory effect on various breast cancer cells.

Materials and methods

Chemical agents and culture conditions

HTMS was synthesized as described previously [21]. Both dimethylsulfoxide (DMSO) and 3-(4,5-dimethylthiazolyl-2)-2,5-diphenyltetrazoliumbromide (MTT) were purchased from Sigma Chemical Co. (St. Louis, MO, USA), while Dulbecco's modified Eagle's medium (DMEM) and the fetal bovine serum (FBS) were purchased from Invitrogen (Grand Island, NY, USA). MCF-7 and MDA-MB-231 cells were grown in low-glucose DMEM supplemented with 5% FBS, while long-term estradiol-deprived (LTED) cells were prepared as previously described and maintained in phenol-free IMEM supplemented with 5% DCC-FBS [26]. The cultures were incubated at 37°C with 5% CO_2.

Cell proliferation assay

The proliferation of MB-231 and MCF-7 cells was determined using an MTT assay, as described previously [27]. Briefly, the cells were seeded at 1×10^4 cells per well into 24-well plates and incubated with HTMS-containing media at 37°C for the desired length of time. Ten microliters of an MTT solution (5 mg/ml) was then added, and the plates were incubated at 37°C for 2 h. To solubilize the MTT formazan crystals, DMSO was added to the cells and the absorbance of the formazan-solubilized DMSO solution read at a wavelength of 595 nm using a microplate reader (Bio-Rad model 550, USA). The vehicle concentrations were <0.1% in all the experiments, which were performed in triplicate. For LTED cell line, the cells were plated in 6-well plates at a density of 60,000 per well in IMEM with 5% DCC. Two days later, the cells were treated with increasing concentrations of HTMS, as indicated in the figure legend, for 5 days with a medium change on day 3. The final vehicle concentration (DMSO) was 0.1%. At the end of the treatment, the cells were rinsed twice with saline. The nuclei were prepared by the sequential addition of 1 ml of HEPES-$MgCl_2$ solution (0.01 mol/l HEPES and 1.5 mmol/l $MgCl_2$) and 0.1 ml of ZAP solution [0.13 mol/l ethylhexadecyldimethylammonium bromide in 3% glacial acetic acid (v/v)], and then counted using a Coulter counter

(Beckmann Coulter, Fullerton, CA). The inhibitory effect of HTMS was compared with that of TMS and doxorubicin in MDA-MB 231 cells as a pilot study.

Apoptotic cell death detection by ELISA assay

To quantitate histone-associated DNA fragments (mono- and oligonucleosomes) in vitro in the cytoplasm of the cells undergoing early apoptosis, $\sim 1 \times 10^4$ cells were seeded in a 24-well plate and incubated with media containing either HTMS or DMSO at 37°C. After 48 h, the floating and adherent cells were collected and analyzed for apoptotic cell death using a Cell Death Detection ELISA^{PLUS} kit (Roche Diagnostics, Mannheim, Germany) according to the manufacturer's instructions. The average values were calculated using the results from three independent assays.

Apoptotic cell death detection by fluorescence microscopy

For the fluorescence microscopy analysis, the cells were washed twice with a 0.01 M PBS buffer (pH 7.4) at every washing step and fixed with a 3.7% paraformaldehyde solution for 10 min at room temperature. The cells (1×10^4 cells per well) were incubated with HTMS (0, 0.3, or 3 μM) for 24 h on an 8-well chamber slide, then washed and fixed. Following incubation with a 0.3% Triton X-100 solution for 15 min, the cells were stained with Alexa fluor 488 phalloidin (molecular probes) for 20 min at room temperature. Meanwhile, to stain the nuclei, the cells were washed and incubated with DAPI (molecular probes) for 2 min at room temperature. The washed cells were then mounted using an anti-fade reagent (molecular

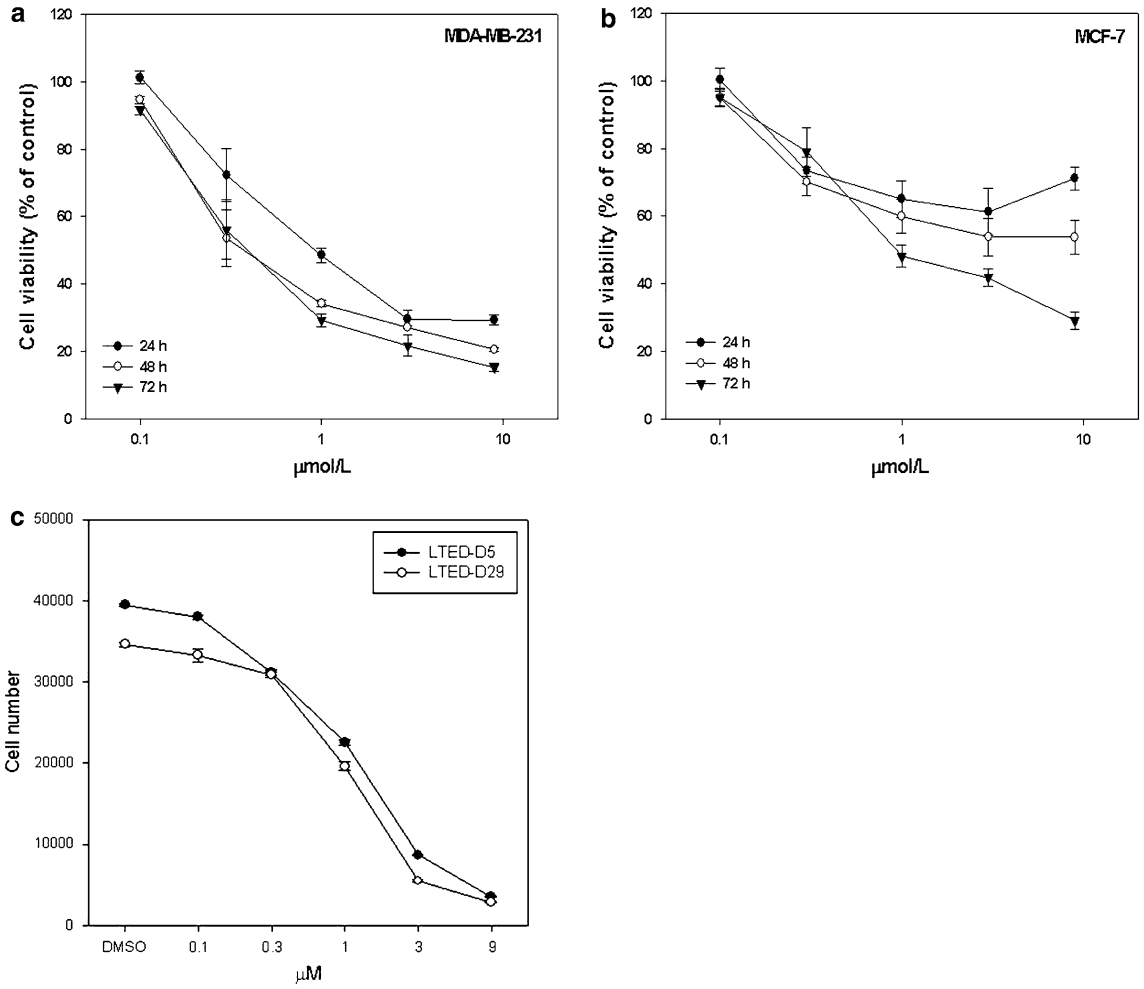

Fig. 2 Growth inhibition of breast cancer cells. Cell survival of MDA-MB-231 (**a**) and MCF-7 cells (**b**) in the presence of the serially diluted HTMS solution (9, 3, 1, 0.3, 0.1 μM) for 24–72 h was determined by MTT assay as described in the "Materials and methods". **c** Inhibitory effect of HTMS on cell growth of long-term estradiol-deprived (LTED) cells. LTED (D5 or D29) cells were plated in six-well plates at a density of 60,000 per well in IMEM containing 5% DCC. The cells were treated with increasing concentration of HTMS for 5 days at which time cell number was determined by counting in a Coulter counter

probes). To detect phosphatidylserine exposure, the cells were incubated with 0.3 μM HTMS for 4 h and then stained with FITC-Annexin V (molecular probes) according to the manufacturer's protocol. The cells were fixed, stained with DAPI, and mounted using an anti-fade reagent. Finally, the cells were analyzed using a Leica DM IRB inverted microscope (Leica Microsystems, Wetzlar, Germany).

Cell cycle analysis by flow cytometry

The changes to the cell cycle progression after exposure to HTMS were investigated based on a fluorescence-activated cell sorting analysis of the propidium iodide (PI)-stained DNA content in the MDA-MB-231 cells treated for 4, 8, 12, 24, and 48 h in the absence or presence of 0.3 μM HTMS. The control and treated floating and adherent cells were collected and counted to 1×10^6. The cells were then washed twice with ice-cold PB, lysed in 1 ml of a DNA staining solution [0.1% sodium citrate, 0.1% Triton X-100, 50 μg/ml of propidium iodide (PI), and 100 μg/ml of RNase A], and incubated at 4°C overnight. For each determination, the DNA content of 20,000 cells was measured using an FACSCalibur flow cytometer (Becton–Dickinson, San Jose, CA), while the percentage of cells in the various phases of the cell cycle was determined using ModFit software (DNA Modeling System, Verity Software House, Inc.).

Measurement of mitochondrial trans-membrane potential

The changes in the mitochondrial trans-membrane potential were determined by fluorescence microscopy using tetramethylrhodamine ethyl ester (TMRE) staining. Briefly, MBA-MB 231 cells were exposed to HTMS (0.3 and 3 μM) for different time periods. Twenty minutes before the end of the incubation period (4 h), a 100 nM TMRE dye was added for mitochondrial matrix staining, while 4,6-diamidino-2-phenylindole (DAPI) was added for nuclear staining. The mitochondrial trans-membrane potential was then measured directly using fluorescence microscopy and compared with a control incubated without HTMS and then stained for 30 min at 37°C.

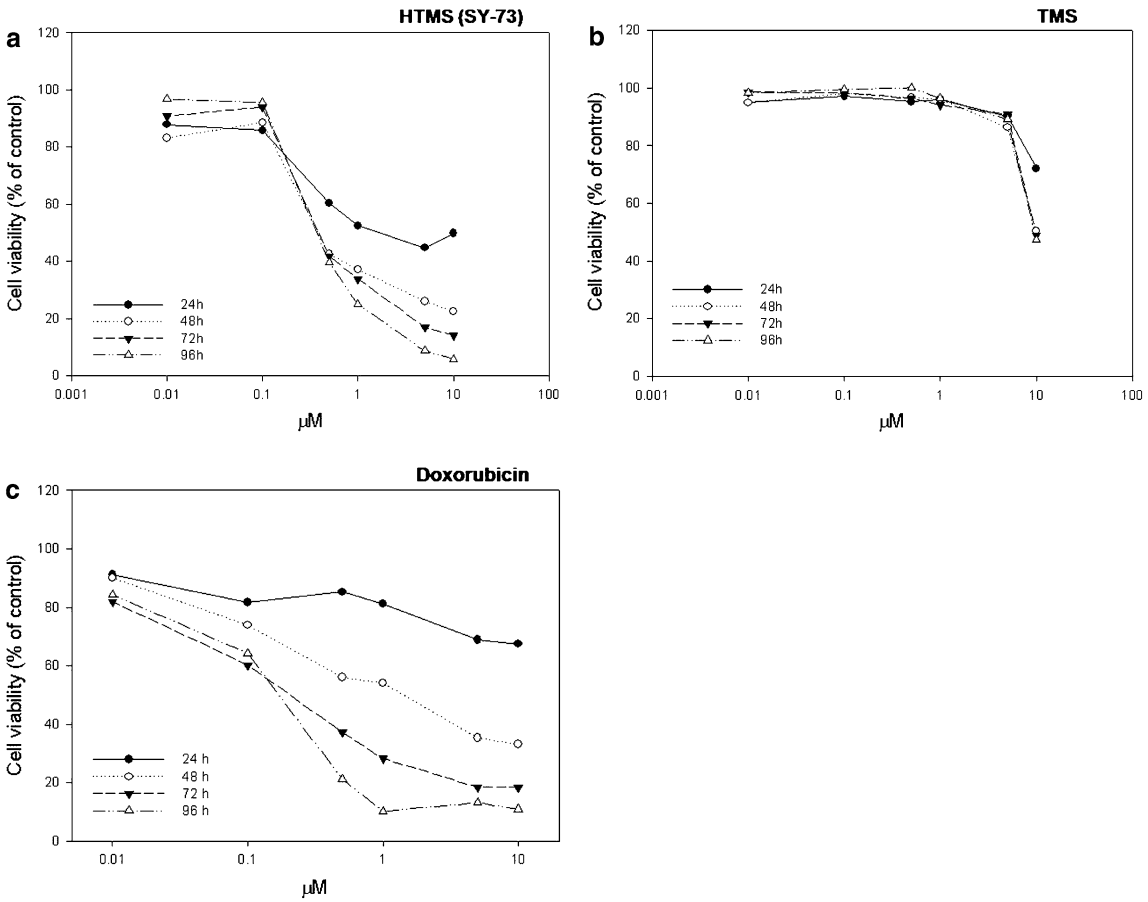

Fig. 3 Comparison of growth inhibition among HTMS, TMS, and doxorubicin in MDA-MB-231 cells in the presence of the serially diluted solution (9, 3, 1, 0.3, 0.1, and 0.01 μM) for 24–96 h was determined by MTT assay

Western blot analysis for cytochrome c and poly (ADP-ribose) polymerase

The cells were grown to a 90% confluence in 6-well plates and then lysed with RIPA buffer (Sigma) including protease inhibitors and phosphatase inhibitors. Thereafter, the protein concentrations of the lysates were determined using a Bradford assay reagent (BioRad, Richmond, CA, USA), and each lysate subjected to a 9–15% SDS polyacrylamide gel, followed by an electrophoretic transfer onto a nitrocellulose membrane (Amersham, Buckinghamshire, UK). The blots were then incubated with a blocking buffer (5% non-fat dried milk solution), while the membrane was probed with primary antibodies dissolved in a 5% non-fat dried milk solution in PBS-T and incubated in PBS-T containing a horseradish peroxidase (HRP)-conjugated secondary antibody. Finally, the bands were identified using an enhanced chemiluminescence (ECL) detection solution (Amersham).

Statistical analysis

The experiments were repeated at least three times, and the results are expressed as the mean ± SEM. The data analysis and graphical visualization were performed using Sigmaplot 10.0 (SPSS Inc.) The differences were considered statistically significant if $P < 0.05$.

Results

HTMS decreased cell viability of breast cancer cells

To evaluate the effect of HTMS on MCF-7 and MDA-MB-231 breast cancer cells, we measured cell viability using the MTT assay after the cells were dose-dependently treated with HTMS. As shown in Fig. 2a and b, continuous exposure to various concentrations of HTMS resulted in a

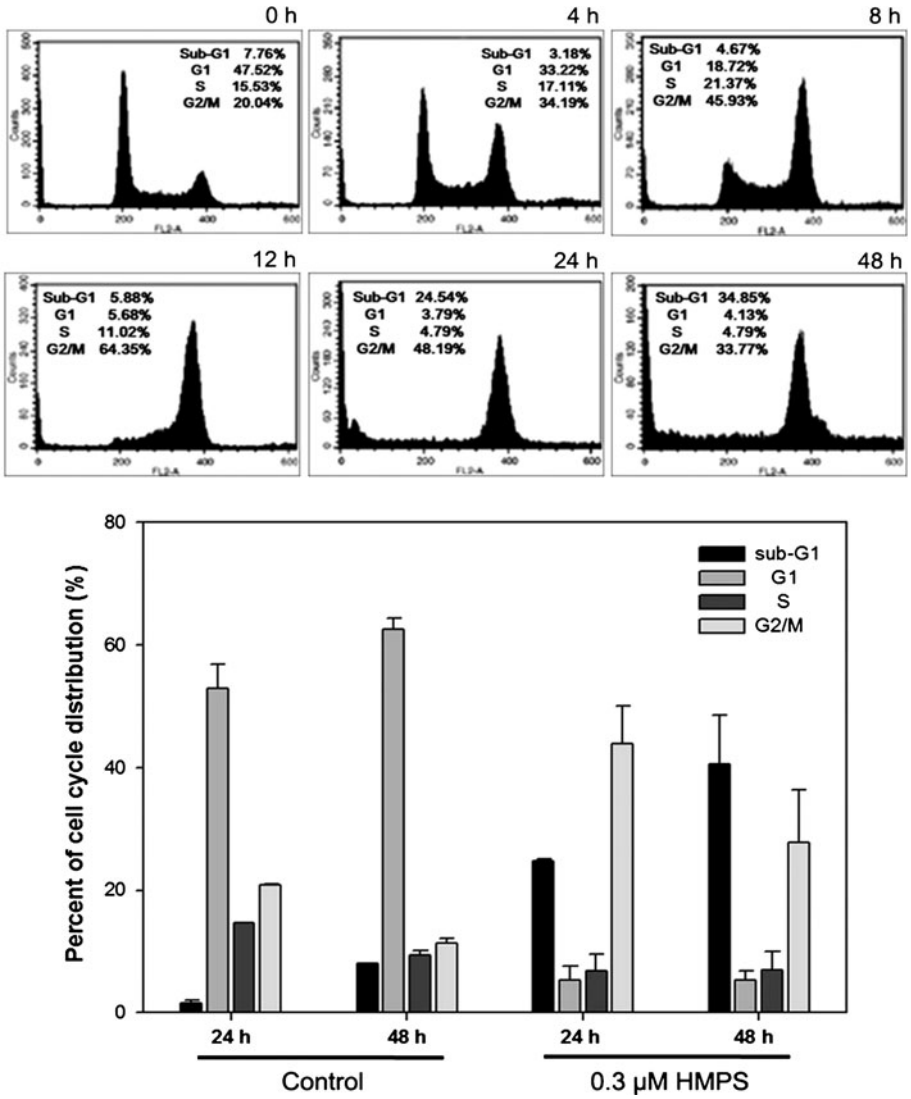

Fig. 4 Cell cycle distribution of MDA-MB-231 cells in the presence of HTMS at several time points analyzed by flow cytometry. After incubation with 0.3 μM HTMS for the desired periods of time, cells were fixed with 70% ethanol and then stained with PI-staining solution containing 50 μg/ml propidium iodide and 100 μg/ml Rnase A. Cells in sub-G1, G1, S, and G2/M of the cell cycle were sorted based on DNA contents using an FACSCalibur system, and 20,000 cells were analyzed from each sample

dose- and time-dependent decrease in cell viability for both cell lines at a concentration over 0.1 μM. In particular, the cell viability of MDA-MB-231 was significantly decreased even after 24 h, while the cell viability of MCF-7 was significantly decreased at 72 h. Interestingly, HTMS significantly inhibited the cell viability at a lower concentration than TMS (1 vs. 10 μM, respectively) and earlier than doxorubicin (24 vs. 48 h, respectively) in MDA-MB-231 cells (Fig. 3). Plus, the number of LTED cells was significantly decreased by HTMS in a dose-dependent manner at ≥0.1 μM (Fig. 2c).

HTMS arrests cell cycle of breast cancer cells in G2/M phase

The effect of HTMS on the cell cycle distribution was analyzed using flow cytometry (Fig. 4). When the MDA-MB-231 cells were treated with 0.3 μM HTMS, the G2/M phase population significantly increased from 20.04 to 64.35% in a time-dependent manner after 12 h, accompanied by a concomitant decrease in the G1 phase cells. The induction of apoptosis by HTMS was also demonstrated by a significant increase in the sub-G1 population, which started to increase after 24 h of HTMS treatment and reached a maximum after 48 h combined with a decrease in the increased G2/M peak.

HTMS induces apoptosis in breast cancer cells

To evaluate the inhibitory mechanism of cell survival by HTMS, an apoptotic cell death assay was conducted via an immunochemical determination of histone-complexed DNA fragments, while fluorescence microscopy was used to detect the apoptotic features of the HTMS-treated cells. As a result, the apoptotic cell death assay showed that apoptosis was effectively induced in both cell lines after 48 h of treatment with HTMS and was more prominent in MCF-7 cells with a high concentration of HTMS (Fig. 5). Meanwhile, the fluorescence microscopy demonstrated extensive nuclear fragmentation with morphological changes in the DAPI-stained cells after 24 h of treatment with HTMS (Fig. 6a). In addition, HTMS-induced apoptosis was also confirmed by FITC-annexin V staining, which showed phosphatidylserine translocation induced by HTMS after 4 h of treatment with 0.3 μM HTMS (Fig. 6b).

Apoptosis by HTMS through mitochondrial cell death pathway

The opening of mitochondrial permeability transition pores (mPTPs), which is consistent with the loss of mitochondrial membrane potential, was monitored using the mitochondrial membrane potential-driven uptake of fluorescent

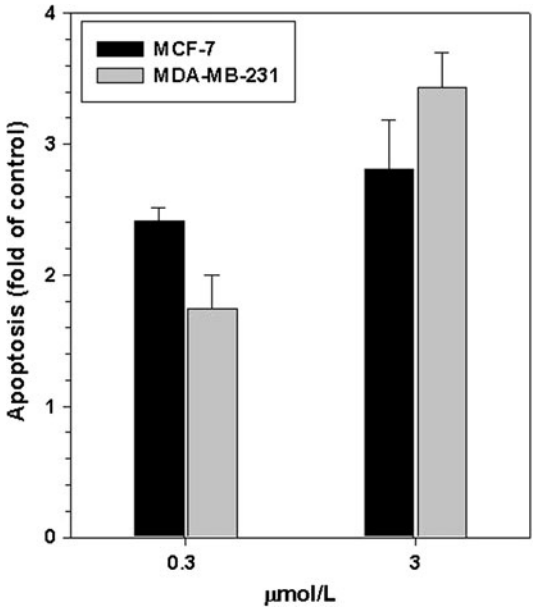

Fig. 5 Apoptotic cell death induced by HTMS was determined by relative quantification of Histone–DNA complex fragments obtained from apoptotic cells after incubation with HTMS for 48 h. Values of apoptosis were set to fold of control not treated with HTMS. The results are the average ± standard error of three independent experiments, and P-value < 0.05 was considered statistically significantly different between control cells and cells treated with HTMS

tetramethylrhodamine ethyl ester (TMRE) [28]. In the MDA-MB-231 cells that were not treated with HTMS, the TMRE dye was localized around the mitochondria, whereas the cells treated with 0.3 μM HTMS for 4 h did not show any TMRE fluorescence around the mitochondria (Fig. 7a). To further clarify the mitochondria-mediated apoptosis induced by HTMS in the MDA-MD-231 cells, the expression of cytosolic and mitochondrial cytochrome c, PARP, and cleaved PARP was measured using a Western blot analysis. After incubation with HTMS for 4 h, the cytochrome *c* levels in the cytosolic fraction increased significantly, whereas the mitochondrial fraction decreased in a dose-dependent pattern (Fig. 7b). In addition, cleaved PARP (89-kDa PARP) was observed, and its protein level increased when increasing the concentration of HTMS (Fig. 7b).

Discussion

The current study found that HTMS can effectively inhibit the growth of various types of breast cancer cells in a dose- and time-dependent manner, characterized by a G2/M arrest of the cell cycle and loss of the mitochondrial membrane potential, resulting in the induction of apoptosis. In particular, the effect of HTMS on apoptosis in vitro was especially dramatic with 80–90% of the cells undergoing

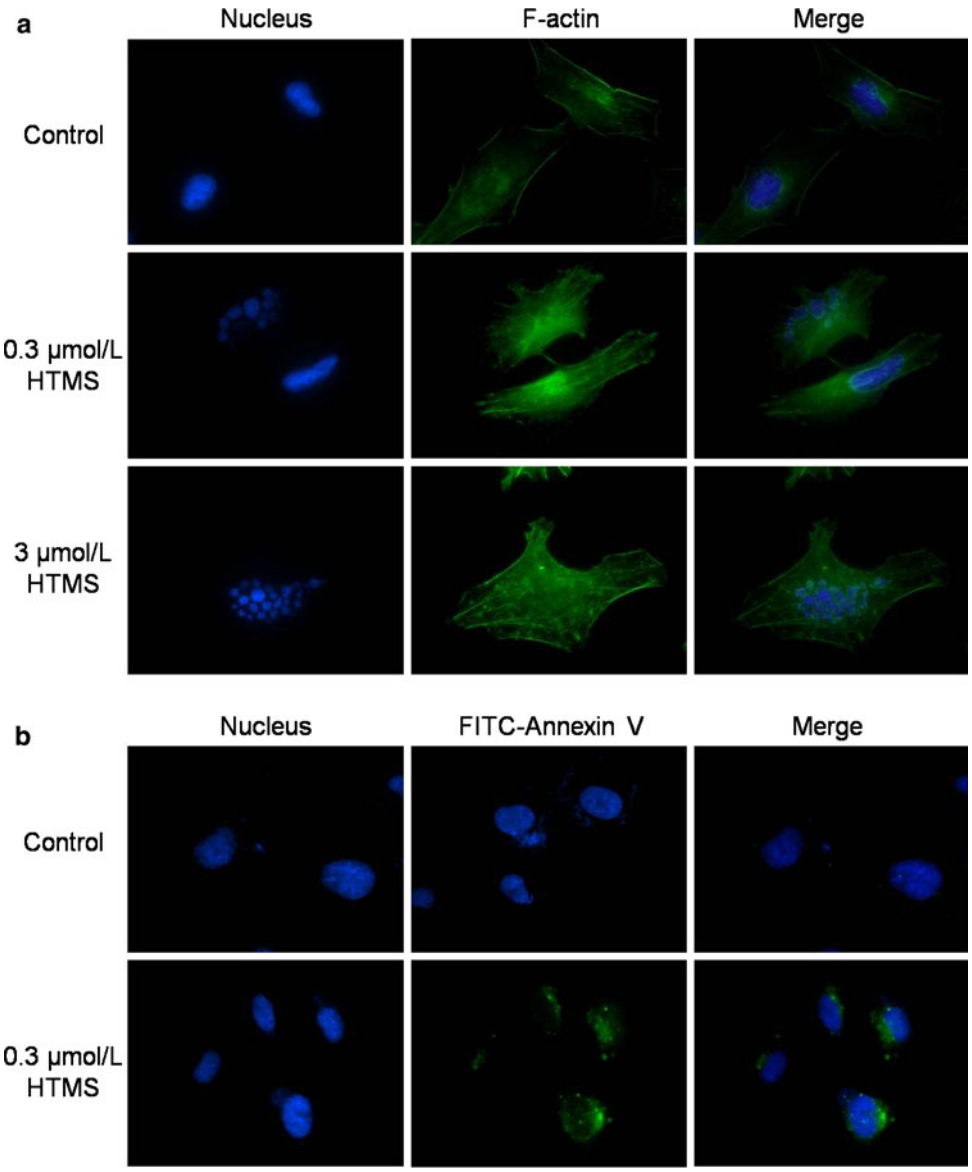

Fig. 6 Fluorescence microscopy for apoptotic nuclear fragmentation and phosphatidylserine exposure. **a** After incubation with HTMS (0, 0.3, 3 μM) for 24 h, the nucleus was detected by DAPI, and F-actin stained by Alexa fluor 488 phalloidin. **b** After 4 h in the absence or presence of 0.3 μM HTMS, the MDA-MB-231 cells were stained with DAPI and FITC-annexin V as described in the section of "Materials and methods"

programmed cell death after 48 h of exposure. Furthermore, the inhibitory effect of HTMS appeared superior to that of TMS in the MDA-MB-231 cell line. Consequently, these results confirm the potential of HTMS as a new therapeutic agent for breast cancers.

HTMS, (*E*)-2-hydroxy-3′,4,5′-trimethoxystilbene, has a similar chemical structure to TMS (2-3′,4,5′-tetramethoxystilbene), a synthetic derivative of the herbal product rhapontigenin. Although TMS was originally developed as an inhibitor of cytochrome P450 1B1, its multiple action effects on breast cancer cells are similar to the HTMS-related mechanisms observed in the current study. Notably, TMS has been demonstrated to inhibit the growth of tamoxifen-resistant breast cancer xenografts in vivo without any evidence of systemic or organ-specific toxicity. In the current study, the cell viability assay showed that 0.3–1 μM HTMS was able to inhibit the growth of the breast cancer cells, whereas 10 μM TMS and 50–100 μM resveratrol are needed to inhibit the proliferation of breast cancer cells [10, 29], indicating that HTMS has a more potent apoptotic effect on breast cancer cells. Meanwhile, cell viability tests demonstrated that MDA-MB-231 cells were more sensitive to HTMS treatment with an early and significant decrease in cell proliferation than MCF-7 cells in this study. Previous studies also demonstrated similar differences in response to new cytotoxic agents between the two cell lines [30, 31]. Generally, ER-negative MDA-MB-231 breast cancer cells are considered as a high grade and more invasive tumor compared with ER-positive MCF-7 cells. As high-grade tumor cells respond rapidly to chemotherapeutic agents, the different response pattern may be related to the difference in growth rate between the two cell lines.

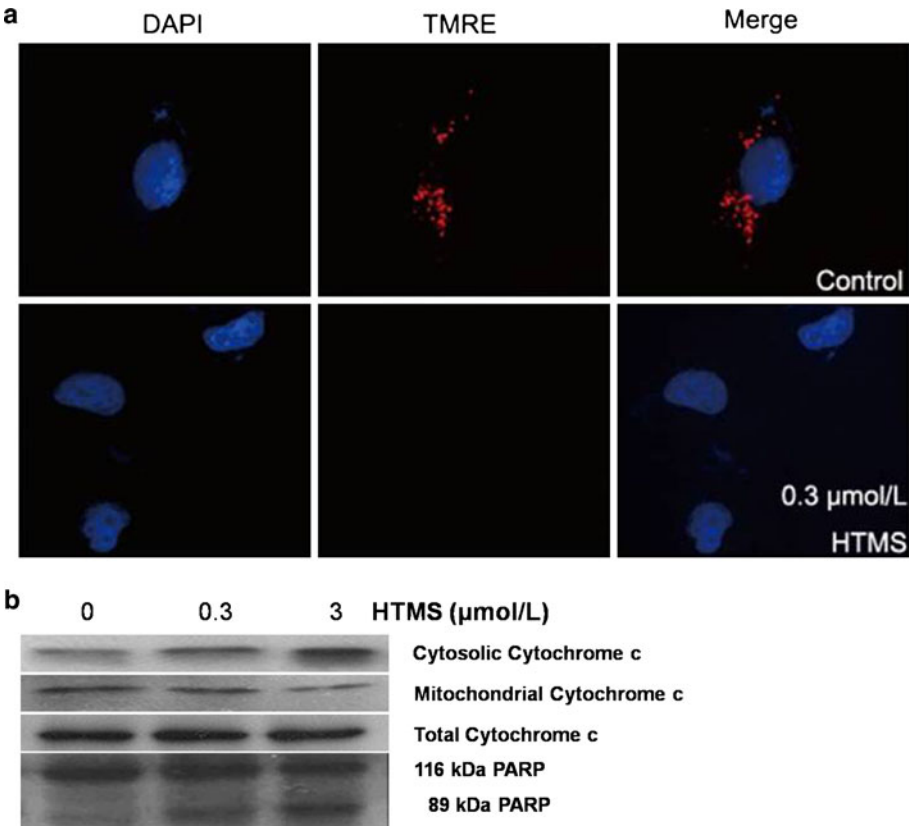

Fig. 7 The depolarization of mitochondrial membrane by HTMS in MDA-MB-231 cells. **a** The changes in mitochondrial membrane potential observed by fluorescence microscopy. At 20 min before the end of the incubation period (4 h), 100 nM tetramethylrhodamine ethyl ester (TMRE) and DAPI were added directly to the cells. After incubation, the cells were fixed with 3.7% paraformaldehyde solution. The stained cells were imaged under a ×64 oil objective. Nuclear staining is shown in blue; TMRE is shown in red. Control implicates the cells incubated without HTMS. **b** Western blot analysis of cytochrome c release and PARP cleavage. After incubation with HTMS for 4 h, cytochrome c levels in cytosolic fraction, mitochondrial fraction, and total lysates. For detection of cleaved PARP, the cells were incubated for 48 h in the presence of HTMS

In apoptotic mammalian cells, several biochemical and morphological features have been observed, including chromatin condensation, nuclear fragmentation, DNA laddering in the nucleus, blebbing of the cell membrane, and the formation of apoptotic bodies in the cytoplasm [32]. Thus, as evidence of HTMS-induced apoptosis, marked morphological changes indicative of cell apoptosis were clearly observed in the current study, including nuclear and cytoplasmic fragmentation, and phosphatidylserine exposure, particularly when the cells were treated with 0.3 μM HTMS for 4 h. In addition, flow cytometry analysis revealed a gradual increase in the number of apoptotic cells and late apoptotic cells among the MBA-MD-231 cells as further evidence of HTMS-induced apoptosis.

To evaluate the role of mitochondria in the HTMS-induced apoptosis, DAPI/TMRE staining demonstrated marked morphologic changes in the disruption of the mitochondrial membrane potential [33–35]. Thus, apoptosis related to an alteration of the mitochondrial membrane potential would appear to be one of the possible mechanisms involved in the HTMS-induced apoptosis of breast cancer cells. In the mitochondria-mediated apoptosis pathway, an apoptotic stimulus is followed by the release of cytochrome c from the mitochondria into the cytosol, which then forms a complex with adenosine triphosphate (ATP) and an apoptotic protease activating factor, leading to the activation of caspase-9 and -3 and the cleavage of the caspase-3 substrate PARP, and eventually to DNA fragmentation and apoptosis [36–38]. Using a Western blot assay, the present study also found that HTMS promoted the release of cytochrome *c* into the cytosol and the cleavage of PARP. Therefore, these findings indicate that HTMS induces apoptosis by activating PARP via the mitochondria-mediated apoptotic pathway.

Another interesting finding from the current study was an increased G2/M peak after HTMS treatment, indicating that HTMS induced a G2/M cell cycle arrest, which is consistent with the results from a previous study, wherein TMS was identified to induce highly abnormal mitotic spindles and multinucleated cells representing an alteration in the mitotic phase of the tumor cells [24]. Thus, similar to TMS, one of the anticancer mechanisms used by HTMS would seem to involve disruption of the mitotic function of the tumor cells.

Although hormone therapy is an effective treatment for ER-positive breast cancer in a postoperative or metastatic state, eventual resistance to hormone therapy remains a major concern. In the current study, HTMS significantly inhibited the growth of LTED human breast cancer cells, known as a hormone-resistant breast cancer cell model that acquires the ability to grow in the absence of estradiol over a long period of time [39]. Therefore, HTMS may be a

potential therapeutic agent for treating hormone-resistant or -refractory breast cancer.

In conclusion, HTMS was shown to possess a significant cell-killing ability for a variety of breast cancer cells based on the induction of apoptosis possibly related to a mitochondria-mediated apoptotic pathway. Moreover, HTMS was also found to cause a G2/M arrest of tumor cells, although the exact mechanism leading to the mitotic arrest remains to be clarified in a future study. Thus, its more potent apoptotic activity toward breast cancer cells when compared with other stilbene analogs makes HTMS a candidate therapeutic agent for treating breast cancers.

Acknowledgments This work was supported by a Korea Science and Engineering Foundation (KOSEF) grant funded by the Korean Government (MEST) (No. 2009-0091573).

References

1. Soleas GJ, Goldberg DM, Grass L, Levesque M, Diamandis EP (2001) Do wine polyphenols modulate p53 gene expression in human cancer cell lines? Clin Biochem 34:415–420
2. Chanvitayapongs S, Draczynska-Lusiak B, Sun AY (1997) Amelioration of oxidative stress by antioxidants and resveratrol in PC12 cells. Neuroreport 8:1499–1502
3. Fauconneau B, Waffo-Teguo P, Huguet F, Barrier L, Decendit A, Merillon JM (1997) Comparative study of radical scavenger and antioxidant properties of phenolic compounds from Vitis vinifera cell cultures using in vitro tests. Life Sci 61:2103–2110
4. Belleri M, Ribatti D, Nicoli S, Cotelli F, Forti L, Vannini V, Stivala LA, Presta M (2005) Antiangiogenic and vascular-targeting activity of the microtubule-destabilizing trans-resveratrol derivative 3, 5, 4′-trimethoxystilbene. Mol Pharmacol 67:1451–1459
5. Jang M, Cai L, Udeani GO, Slowing KV, Thomas CF, Beecher CW, Fong HH, Farnsworth NR, Kinghorn AD, Mehta RG, Moon RC, Pezzuto JM (1997) Cancer chemopreventive activity of resveratrol, a natural product derived from grapes. Science 275:218–220
6. Bhat KP, Pezzuto JM (2002) Cancer chemopreventive activity of resveratrol. Ann N Y Acad Sci 957:210–229
7. Blumenstein I, Keseru B, Wolter F, Stein J (2005) The chemopreventive agent resveratrol stimulates cyclic AMP-dependent chloride secretion in vitro. Clin Cancer Res 11:5651–5656
8. Dong Z (2003) Molecular mechanism of the chemopreventive effect of resveratrol. Mutat Res 523–524:145–150
9. Lu R, Serrero G (1999) Resveratrol, a natural product derived from grape, exhibits antiestrogenic activity and inhibits the growth of human breast cancer cells. J Cell Physiol 179:297–304
10. Scarlatti F, Sala G, Somenzi G, Signorelli P, Sacchi N, Ghidoni R (2003) Resveratrol induces growth inhibition and apoptosis in metastatic breast cancer cells via de novo ceramide signaling. Faseb J 17:2339–2341
11. Garvin S, Ollinger K, Dabrosin C (2006) Resveratrol induces apoptosis and inhibits angiogenesis in human breast cancer xenografts in vivo. Cancer Lett 231:113–122
12. Pozo-Guisado E, Merino JM, Mulero-Navarro S, Lorenzo-Benayas MJ, Centeno F, Alvarez-Barrientos A, Fernandez-Salguero PM (2005) Resveratrol-induced apoptosis in MCF-7 human breast cancer cells involves a caspase-independent mechanism with downregulation of Bcl-2 and NF-kappaB. Int J Cancer 115:74–84
13. Alkhalaf M (2007) Resveratrol-induced growth inhibition in MDA-MB-231 breast cancer cells is associated with mitogen-activated protein kinase signaling and protein translation. Eur J Cancer Prev 16:334–341
14. Marier JF, Vachon P, Gritsas A, Zhang J, Moreau JP, Ducharme MP (2002) Metabolism and disposition of resveratrol in rats: extent of absorption, glucuronidation, and enterohepatic recirculation evidenced by a linked-rat model. J Pharmacol Exp Ther 302:369–373
15. Asensi M, Medina I, Ortega A, Carretero J, Bano MC, Obrador E, Estrela JM (2002) Inhibition of cancer growth by resveratrol is related to its low bioavailability. Free Radic Biol Med 33:387–398
16. Walle T, Hsieh F, DeLegge MH, Oatis JE Jr, Walle UK (2004) High absorption but very low bioavailability of oral resveratrol in humans. Drug Metab Dispos 32:1377–1382
17. Roberti M, Pizzirani D, Simoni D, Rondanin R, Baruchello R, Bonora C, Buscemi F, Grimaudo S, Tolomeo M (2003) Synthesis and biological evaluation of resveratrol and analogues as apoptosis-inducing agents. J Med Chem 46:3546–3554
18. Peter Guengerich F, Chun YJ, Kim D, Gillam EM, Shimada T (2003) Cytochrome P450 1B1: a target for inhibition in anticarcinogenesis strategies. Mutat Res 523–524:173–182
19. Ovesna Z, Horvathova-Kozics K (2005) Structure-activity relationship of trans-resveratrol and its analogues. Neoplasma 52:450–455
20. Soares DG, Andreazza AC, Salvador M (2003) Sequestering ability of butylated hydroxytoluene, propyl gallate, resveratrol, and vitamins C and E against ABTS, DPPH, and hydroxyl free radicals in chemical and biological systems. J Agric Food Chem 51:1077–1080
21. Kim S, Ko H, Park JE, Jung S, Lee SK, Chun YJ (2002) Design, synthesis, and discovery of novel trans-stilbene analogues as potent and selective human cytochrome P450 1B1 inhibitors. J Med Chem 45:160–164
22. Roupe KA, Remsberg CM, Yanez JA, Davies NM (2006) Pharmacometrics of stilbenes: seguing towards the clinic. Curr Clin Pharmacol 1:81–101
23. Ma Z, Molavi O, Haddadi A, Lai R, Gossage RA, Lavasanifar A (2008) Resveratrol analog trans 3, 4, 5, 4′-tetramethoxystilbene(DMU-212) mediates anti-tumor effects via mechanism different from that of resveratrol. Cancer Chemother Pharmacol 63:27–35
24. Park H, Aiyar SE, Fan P, Wang J, Yue W, Okouneva T, Cox C, Jordan MA, Demers L, Cho H, Kim S, Song RX, Santen RJ (2007) Effects of tetramethoxystilbene on hormone-resistant breast cancer cells: biological and biochemical mechanisms of action. Cancer Res 67:5717–5726
25. Kim S, Min SY, Lee SK, Cho WJ (2003) Comparative molecular field analysis study of stilbene derivatives active against A549 lung carcinoma. Chem Pharm Bull (Tokyo) 51:516–521
26. Santen R, Jeng MH, Wang JP, Song R, Masamura S, McPherson R, Santner S, Yue W, Shim WS (2001) Adaptive hypersensitivity to estradiol: potential mechanism for secondary hormonal responses in breast cancer patients. J Steroid Biochem Mol Biol 79:115–125
27. Dell'Erba C, Chiavarina B, Fenoglio C, Petrillo G, Cordazzo C, Boncompagni E, Spinelli D, Ognio E, Aiello C, Mariggio MA, Viale M (2005) Inhibition of cell proliferation, cytotoxicity and induction of apoptosis of 1, 4-bis (1-naphthyl)-2, 3-dinitro-1, 3-butadiene in gastrointestinal tumour cell lines and preliminary evaluation of its toxicity in vivo. Pharmacol Res 52:271–282
28. Drummond RM, Mix TC, Tuft RA, Walsh JV Jr, Fay FS (2000) Mitochondrial Ca^{2+} homeostasis during Ca^{2+} influx and Ca^{2+} release in gastric myocytes from Bufo marinus. J Physiol 522(Pt 3):375–390

29. Tang HY, Shih A, Cao HJ, Davis FB, Davis PJ, Lin HY (2006) Resveratrol-induced cyclooxygenase-2 facilitates p53-dependent apoptosis in human breast cancer cells. Mol Cancer Ther 5:2034–2042
30. Billam M, Sobolewski MD, Davidson NE (2009) Effects of a novel DNA methyltransferase inhibitor zebularine on human breast cancer cells. Breast Cancer Res Treat 120:581–592
31. Zhang N, Kong X, Yan S, Yuan C, Yang Q (2010) Huaier aqueous extract inhibits proliferation of breast cancer cells by inducing apoptosis. Cancer Sci 101:2375–2383
32. Okada H, Mak TW (2004) Pathways of apoptotic and non-apoptotic death in tumour cells. Nat Rev Cancer 4:592–603
33. Hirsch T, Marzo I, Kroemer G (1997) Role of the mitochondrial permeability transition pore in apoptosis. Biosci Rep 17:67–76
34. Scarlett JL, Sheard PW, Hughes G, Ledgerwood EC, Ku HH, Murphy MP (2000) Changes in mitochondrial membrane potential during staurosporine-induced apoptosis in Jurkat cells. FEBS Lett 475:267–272
35. Precht TA, Phelps RA, Linseman DA, Butts BD, Le SS, Laessig TA, Bouchard RJ, Heidenreich KA (2005) The permeability transition pore triggers Bax translocation to mitochondria during neuronal apoptosis. Cell Death Differ 12:255–265
36. Green DR, Reed JC (1998) Mitochondria and apoptosis. Science 281:1309–1312
37. Gogvadze V, Orrenius S, Zhivotovsky B (2006) Multiple pathways of cytochrome c release from mitochondria in apoptosis. Biochim Biophys Acta 1757:639–647
38. Scovassi AI, Poirier GG (1999) Poly(ADP-ribosylation) and apoptosis. Mol Cell Biochem 199:125–137
39. Jeng MH, Shupnik MA, Bender TP, Westin EH, Bandyopadhyay D, Kumar R, Masamura S, Santen RJ (1998) Estrogen receptor expression and function in long-term estrogen-deprived human breast cancer cells. Endocrinology 139:4164–4174